A Coarse-Grained Molecular Dynamics Investigation on Spontaneous Binding of Aβ_{9-40} Fibril with Cholesterol-mixed DPPC Bilayer

Nikhil Agrawal[1,2]*, Adam A Skelton[2], Emilio Parisini[1,3]*

[1]Latvian Institute of Organic Synthesis, Aizkraukles 21, LV, Riga 1006, Latvia

[2]College of Health Sciences, University of KwaZulu-Natal, Durban, South Africa

[3]Department of Chemistry "G. Ciamician", University of Bologna, Bologna, Italy

***corresponding authors:** nikhil.08oct@gmail.com, (N. Agrawal), emilio.parisini@osi.lv (E. Parisini)

Abstract

Alzheimer's disease is the most common form of dementia. Its aetiology is characterized by misfolding and aggregation of amyloid-β (Aβ) peptides into β-sheet-rich Aβ oligomers/fibrils. Whereas experimental studies have suggested that Aβ oligomers/fibrils interact with the cell membranes and perturb their structures and dynamics, the molecular mechanism of this interaction is still not fully understood. In the present work, we have performed a total of 8 μs-long simulations of an Aβ_{9-40} fibril hexamer with a cholesterol-rich DPPC bilayer. Our simulation data captures the spontaneous binding of the aqueous Aβ_{9-40} fibril hexamer with the membrane and shows that both the middle region and the C-terminal residues of the fibril play an important role in this event. A decrease in the number of water molecules around the Aβ_{9-40} fibril and an increase in the number of lipids occurs as the distance between the Aβ_{9-40} fibril and the membrane decreases. We also detected that binding of the Aβ_{9-40} fibril appears to cause the localized thinning of the membrane at the point of contact. The identified binding residues of the Aβ fibril could serve as a potential target region for the design of new inhibitors, thus opening new avenues in structure-based drug design against Aβ oligomer/fibril-membrane interaction.

Keywords: Alzheimer's disease, Amyloid, cholesterol, DPPC, Lipid membrane, MD simulations

Introduction

Amyloid fibrils are misfolded β-sheet-rich aggregated proteins that play a key role in more than 20 diseases, including Alzheimer's disease (AD), Parkinson's disease (PD), type 2 diabetes, HIV, and different forms of systemic amyloidosis [1-4]. Conditions involving amyloid fibrils formation are commonly known as protein misfolding diseases, which affect millions of people around the world [5, 6]. According to the amyloid cascade hypothesis, in the brain of AD patients the amyloid β peptide (Aβ) undergoes conformational changes to form water-insoluble Aβ fibrils [7, 8]. These Aβ fibrils then form extracellular neuronal plaques, which represent the major pathological hallmark of AD [9, 10].

Several studies have been performed previously using different experimental techniques to reveal the effect of the interaction between Aβ fibrils and lipids/membranes. Han *et al.* [11], used electron tomography to visualize the interaction of Aβ fibrils with lipids of different sizes, also reporting that intracellular fibrils deform the structure of intracellular lipid vesicles and puncture through the vesicular membrane into the cytoplasm. Using simultaneous coherent anti-Stokes Raman scattering (CARS) and 2-photon fluorescence microscopy Kiskis *et al.* [12] showed that lipids co-localize with fibrillar β-amyloid (Aβ) plaques. In another experimental study, Burns *et al.* [13] revealed the co-localization of cholesterol in Aβ plaques. Previously, several MD simulations studies were also done to investigate the interaction between membranes and Aβ oligomers/fibrils. For instance, Yu *et al.* [14] performed MD simulations of the interaction between $A\beta_{17-42}$ fibrils and a mixed anionic POPC–POPG bilayer. Their study showed that anionic lipids play an important role in the absorption of the $A\beta_{17-42}$ pentamer in the membrane. Tofoleanu *et al.* [15] conducted MD simulations of the interaction between Aβ fibrils and a POPE lipid bilayer, and their data revealed that the charged residues Glu22, Asp23 and Lys28 form electrostatic interactions with head group atoms of the lipid. In another study, Tofoleanu *et al.* [16] used MD simulations to investigate the behaviour of Aβ fibrils with POPC and POPE bilayers. The study revealed that Aβ fibrils form short-lived contacts with POPC head groups and strong contacts with POPE head groups. Dong *et al.* [17] performed MD simulations of $A\beta_{40}$ fibril trimers with a POPG bilayer, revealing that their interaction is mediated by the N-terminal β-sheet. In a recent work, Dias *et al.* [18] used coarse-grained (CG) simulations to show the binding of $A\beta_{1-42}$ fibrils with a cholesterol-rich phosphatidylcholine (PC) bilayer, showing that 30% cholesterol is optimal for $A\beta_{1-42}$ fibril interaction with the membrane and that

increasing the cholesterol content in PC bilayer up to 50% does not increase the binding frequency of $A\beta_{1-42}$ fibrils with the membrane.

It is well established that Aβ fibrils are highly polymorphic in nature and that their two isoforms, $A\beta_{40}$ and $A\beta_{42}$, feature different structures at the molecular level [19]. Hence, it is important to investigate also the interaction of $A\beta_{40}$ fibrils with lipid membranes. In the present study, we aimed to capture the spontaneous binding of the $A\beta_{40}$ fibril hexamer in a mixed 70% DPPC and 30% cholesterol bilayer. To this end, we have performed four independent coarse-grained MD simulations for a total of 8 μs (2 μs each), which have allowed us to investigate whether $A\beta_{40}$ fibrils spontaneously bind to a cholesterol-rich bilayer, which amino acids are involved in the process and how this affects fibril solvation and the thickness of the bilayer.

Methods

Structure and force field of $A\beta_{9-40}$ hexamer fibril and DPPC-cholesterol membrane

To perform CG molecular dynamics simulations, we used the NMR structure of the $A\beta_{9-40}$ fibril hexamer (PDB id: 2LMN). The $A\beta_{9-40}$ fibril structure contains two β-sheets (residue 13-19 and residue 32-40)[20]. The atomistic structure (Figure 1A) was converted into the CG model (Figure 1B) using the CHARMM-GUI Martini maker [21, 22].

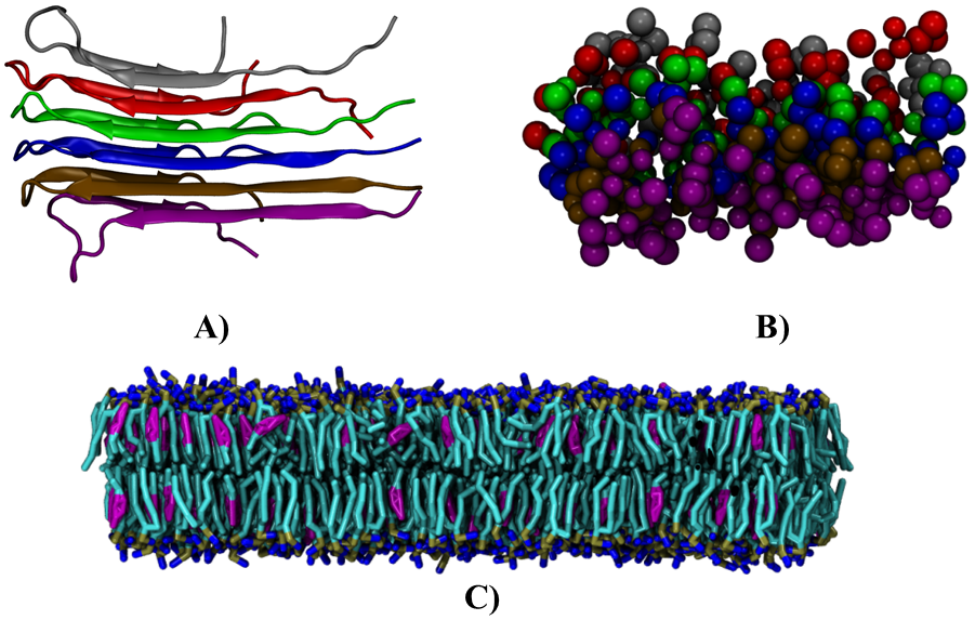

Figure 1. A) NMR structure of $A\beta_{9-40}$ fibril (PDB id: 2LMN). B) CG model of $A\beta_{9-40}$ fibril. C) Cholesterol-mixed DPPC bilayer.

The initial structure of DPPC-cholesterol was downloaded from the Martini Lipid database, which is available on the Martini CG website (http://www.cgmartini.nl/index.php/example-applications2/lipid-membranes). To transform it into a larger patch of membrane, the DPPC-cholesterol structure was replicated in the x and y-direction using the GROMACS genconf program. The mixed bilayer contains 1368 DPPC (~70 %) molecules and 576 (~30%) cholesterol molecules (Figure 1C). The Martini 2.2 protein force field [23] was used for the $A\beta_{9-40}$ hexamer, and the Martini 2.0 force field was used for the membrane, water and ions [24].

Simulation protocol

In our simulation, the final system featured one $A\beta_{9-40}$ hexamer, a DPPC-cholesterol bilayer and 107194 water molecules. To neutralize the system, 6 Na^+ ions were added. Initially, to minimize the energy of the systems, 5000 steps of steepest descent [25] were performed, followed by a 30 ns equilibration using canonical ensemble (NVT) and by 100 ns equilibration using the isobaric-isothermal ensemble (NPT). The production run was done using the NPT ensemble. The Berendsen algorithm [26] was used for pressure coupling and the velocity-rescale algorithm [27] was used for temperature coupling. Pressure coupling and temperature bath times were set at 5.0 and 1.0 ps, respectively. All simulations were performed at a temperature of 303.15 K and 1 atm pressure. The Particle mesh Ewald (PME) algorithm [28] was used for long-range electrostatic interactions while van der Waals (vdW) interactions were calculated using the switch function from 9 to 12 Å; a 20 fs time step was used for the integration of Newton's equations of motion.

A total of 4 independent simulations were done using an initial random velocity generated by GROMACS [29]. The simulation time of each trajectory was 2 μs.

Analysis details

The minimum distance of the $A\beta_{9-40}$ fibril residues from the membrane was calculated using the GROMACS minidist program. The interaction energy between the $A\beta_{9-40}$ fibril and the membrane was calculated using the GROMACS MDRUN program with the "rerun" option. An interaction with a $A\beta_{9-40}$ fibril residue was taken into account when the minimum distance between membrane lipids (DPPC/cholesterol) and the residue was less than 6 Å. The

minimum distance between each residue and the membrane was calculated between 1μs to 2 μs. The number of water and lipid molecules was calculated within 6 Å of the Aβ9-40 fibril. The thickness of the bilayer was calculated using the g_thickness tool [30] at four different time points (0-0.1 μs, 0.4-0.5 μs, 1.4-1.5 μs, and 1.9-2.0 μs)

Results

Binding of the $A\beta_{9-40}$ fibril with the membrane:

Cytotoxicity of Amyloid fibrils is generally reported to their binding with cell membranes [31, 32]. To see the spontaneous binding of aqueous $A\beta_{9-40}$ fibrils with the membrane, we calculated the time evolution of the minimum distance and of the interaction energy between the protein and the membrane. Out of a total of 4 independent trajectories, we observed spontaneous binding of the $A\beta_{9-40}$ fibrils in two trajectories (SIM3 and SIM4). In the other two trajectories (SIM1 and SIM2), only a negligible number of contacts was observed. Figure 2A shows the time evolution of the minimum distance between $A\beta_{9-40}$ fibril and the membrane. In all trajectories, we noticed that the distance between the $A\beta_{9-40}$ fibril and the membrane decreased within the initial 0.4 μs. Figure 3 shows the distance between the $A\beta_{9-40}$ fibril and the membrane at three different time points as derived from SIM4. In the case of SIM1 and SIM2, the $A\beta_{9-40}$ fibril remained at a distance of ~20Å from the membrane for most of the last 1μs of the simulation time. However, in the case of SIM3 and SIM4, the minimum distance of the $A\beta_{9-40}$ fibril from the membrane was around ~0Å in the last 1μs of the simulation time, which shows that in both these simulations the $A\beta_{9-40}$ fibril remained stably bound to the membrane. To evaluate the interaction energy profile of the system, we plotted the time evolution of the interaction energy between the membrane and the $A\beta_{9-40}$ fibril for all four trajectories (Figure 2B). This analysis showed that interactions between the $A\beta_{9-40}$ fibril and the membrane took place mainly in SIM3 and SIM4. In the case of SIM3, the interaction energy began to decrease around ~0.8 μs and fluctuated between ~-600 and ~-800 kJ/mol for the rest of the simulation time. In SIM4, the interaction energy decreased in two steps: in the first step (~0.5 μs), the interaction energy became favourable and fluctuated between ~-700 to -800 kJ/mol and in the second step (~1.5 μs), the interaction energy further decreased, becoming more favourable (~-1000 kJ/mol). Overall, this data suggest that an $A\beta_{9-40}$ fibril can spontaneously bind to a cholesterol-rich DPPC bilayer and that the binding of the $A\beta_{9-40}$ fibril with the membrane is energetically favourable.

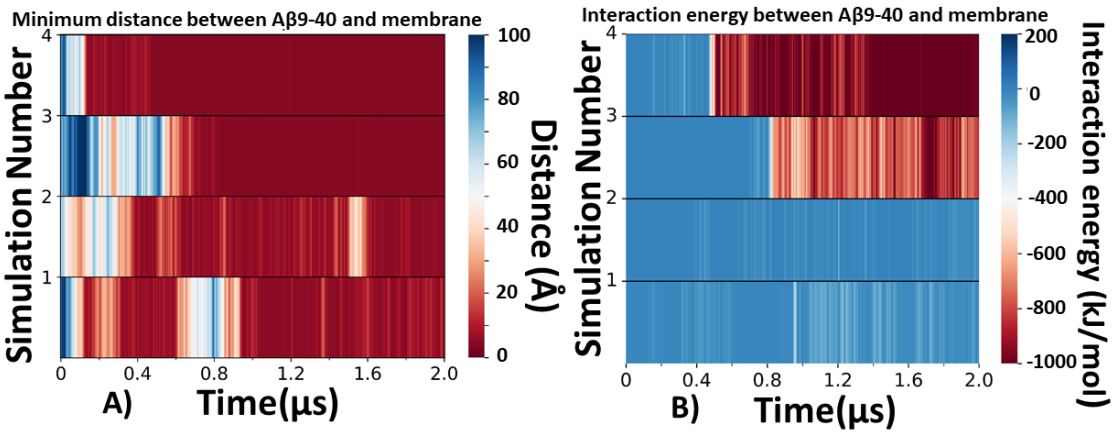

Figure 2. A) Time evolution of the minimum distance between the Aβ9-40 fibril and the membrane B) Time evolution of the interaction energy between the Aβ9-40 fibril and the membrane.

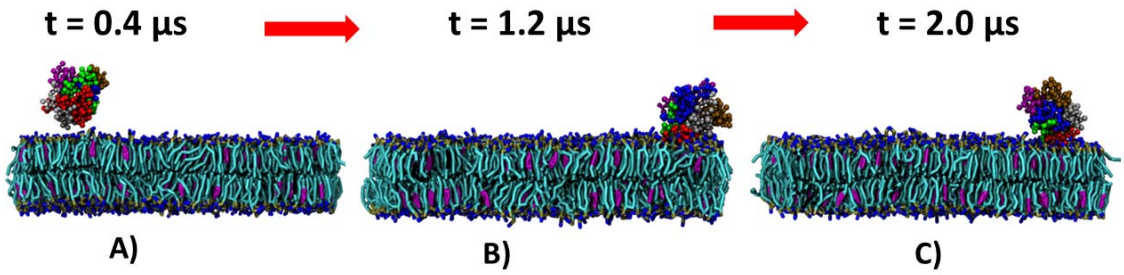

Figure 3. Structures of the $A\beta_{9\text{-}40}$ fibril at three different time points taken from the SIM4 trajectory. A) Representative image at 0.4 μs. B) Representative image at 1.2 μs. C) Representative image at 2.0 μs. Each chain of the protein is shown in a different colour: chain A silver, chain B red, chain C green, chain D blue, chain E ochre and chain F purple. Protein beads are shown using a van der Waals representation while the membrane is shown in Licorice. DPPC lipid molecules are shown in cyan and cholesterol molecules are shown in maroon.

Identification of Membrane Binding residues

To identify those residues that bind to the membrane, we calculated the percentage of simulation time (from 1μs to 2μs) for which the minimum of each residue's distance from the membrane was less than 6Å (Figure 4). In SIM1 and SIM2, negligible contacts were formed between the membrane and the $A\beta_{9\text{-}40}$ fibril except for four residues (Figure 4, A and B). In the case of SIM3 and SIM4, a significant number of contacts between residues and the membrane was observed (Figure 4, C and D). In SIM3, chain A residues Lys16, Leu17, Val18, Phe19, Phe20, Lys28, Ile31, Ile32 Gly33, Leu34, Met35, Val36, Gly37, Gly38, Val39, and, Val40 formed contacts with the membrane for more than 80% of the simulation time. In SIM4, chain B and chain C residues formed major contacts with the membrane. In particular, chain B residues Lys16, Leu17, Val18, Phe19, Phe20, Glu22, Ile31, Ile32, Leu34, Met35,

Val36, Val39, and, Val40 and chain C residues Ile31, Ile32, Leu34, Met35, Val36, Val39, and Val40 formed contacts for 80% or more of the simulation time. Overall, this data suggests that in SIM3 and SIM4 a set of similar residues interacted with the membrane for a long period of time, and that both charged and hydrophobic residues played an important role in the binding of the $A\beta_{9\text{-}40}$ fibril to the membrane.

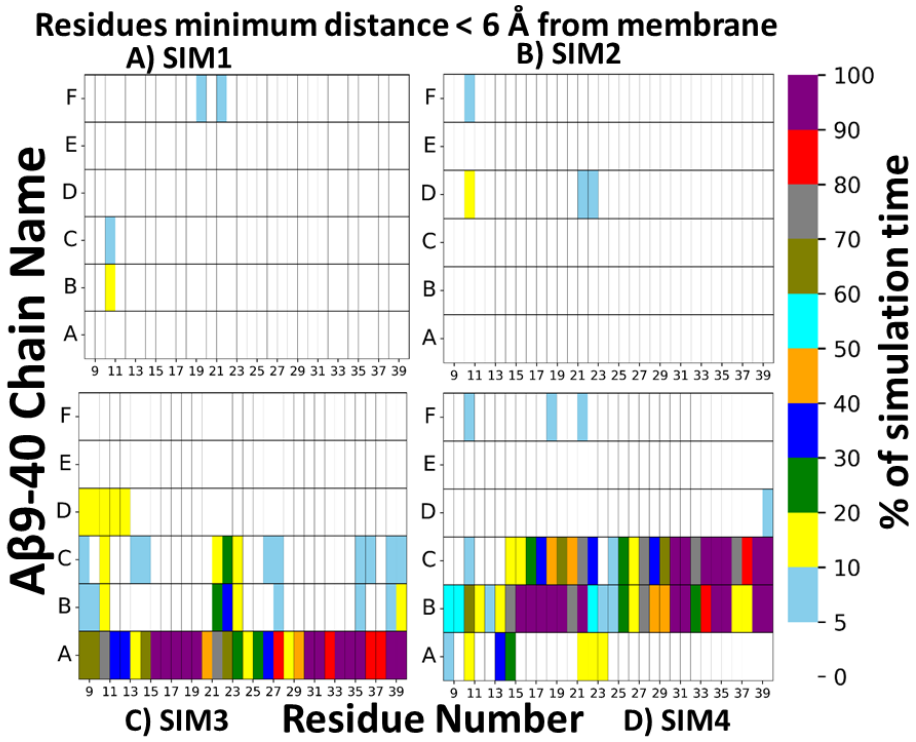

Figure 4. A) Percentage of time residues remained within 6Å of the membrane for the last 1 µs of the simulation time in SIM1 B) Percentage of time residues remained within 6Å of the membrane for the last 1 µs of the simulation time in SIM2 C) Percentage of time residues remained within 6Å of the membrane for the last 1 µs of the simulation time in SIM3 D) Percentage of time residues remained within 6Å of the membrane for the last 1 µs of the simulation time in SIM4.

Time evolution of the number of water, lipid molecules around $A\beta_{9\text{-}40}$ fibril

To quantify the number of water molecules that the $A\beta_{9\text{-}40}$ fibril has to displace to interact with the membrane, we calculated the time evolution of the number of water molecules within 6Å of the $A\beta_{9\text{-}40}$ fibril for all four independent trajectories (Figure 5). As the distance between the membrane and the $A\beta_{9\text{-}40}$ fibril decreased, a significant change in $A\beta_{9\text{-}40}$ fibril solvation occurred. While displacement of water molecules around the $A\beta_{9\text{-}40}$ fibril took place

within the initial ~500 ns in all the simulation trajectories, this was more pronounced in SIM3 after ~850 ns, and in SIM4 after ~1400 ns. Indeed, between ~100 and ~120 water molecules were displaced in SIM3 and SIM4, which is when we observed the maximum number of contacts between the $A\beta_{9\text{-}40}$ fibril and the membrane (Figure: 6A). To quantify how many lipid molecules were found in proximity of the $A\beta_{9\text{-}40}$ fibril, we calculated the time evolution of the number of lipid molecules for all four trajectories. In SIM1 and SIM2, we observed that there were less than 5 lipid molecules at a distance shorter than 6 Å from any residue of the $A\beta_{9\text{-}40}$ fibril for most of the simulation time. In SIM3 and SIM4, an increase in the number of lipid molecules near the $A\beta_{9\text{-}40}$ fibril was found to occur concomitantly with a decrease in $A\beta_{9\text{-}40}$ fibril solvation, thus showing that loss of water molecules in both these simulations takes place as contacts with the membrane are formed. In SIM3 and SIM4, there were on average ~10 to ~15 lipid molecules within 6 Å of $A\beta_{9\text{-}40}$ fibril once it formed contacts with the membrane, in a few instances up to ~20. Overall, this data suggests that in order to move spontaneously from an aqueous environment, the $A\beta_{9\text{-}40}$ fibril has to displace a significant amount of water molecules so that it can interact with 10 or more lipid molecules.

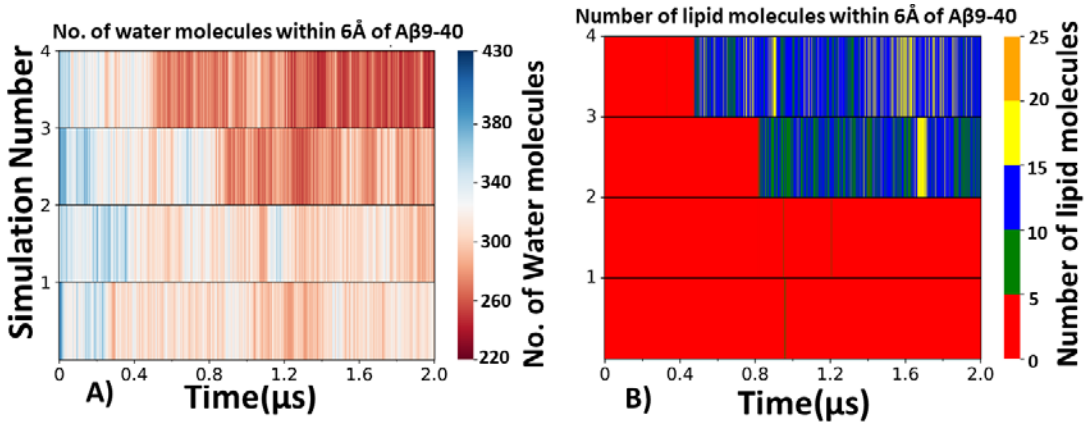

Figure 5. A) Time evolution of the number of water molecules within 6Å of the $A\beta_{9\text{-}40}$ fibril. B) Time evolution of the number of lipid molecules within 6Å of the $A\beta_{9\text{-}40}$ fibril.

<u>Time evolution of the number of contacts between Aβ9-40 fibril and membrane lipids</u>

To assess how many contacts were formed between the $A\beta_{9\text{-}40}$ fibril and the membrane, we calculated the time evolution of the number of contacts for all four independent trajectories. The number of actual contacts was calculated taking into consideration any minimum distance shorter than 6 Å between the $A\beta_{9\text{-}40}$ fibril and lipids. There was an almost insignificant number of contacts formed between the membrane and the $A\beta_{9\text{-}40}$ fibril in SIM1 and SIM2. In SIM3 and SIM4, a sudden increment in the number of contacts was observed at

time points ~0.8 µs and ~0.4 µs, respectively. In SIM4, the number of contacts ranged between ~100 to ~200 from ~0.4 µs to ~1.5 µs while, thereafter, the number of contacts increased between ~150 and ~220 for the rest of the simulation time. In SIM3, after ~0.8 µs the number of contacts fluctuated between ~100 and ~150 for most of the remaining simulation time, although a small further increment in contacts was observed for a short period of time at around ~1.7 µs. To further understand the individual contribution of each lipid in the interaction between the $A\beta_{9\text{-}40}$ fibril and the membrane, we calculated the number of contacts with both DPPC and cholesterol individually (Figure 5, B and C). While the major contribution to contacts came from DPPC, cholesterol also contributed significantly to the total number of contacts in both SIM3 and SIM4. Since there are ~70% DPPC lipids in the membrane, it was expected that DPPC would contribute the highest number of contacts. Figure 5D shows chain A residues interacting with the membrane in SIM3 for more than 80% of the simulation time in the range 1-2 µs.

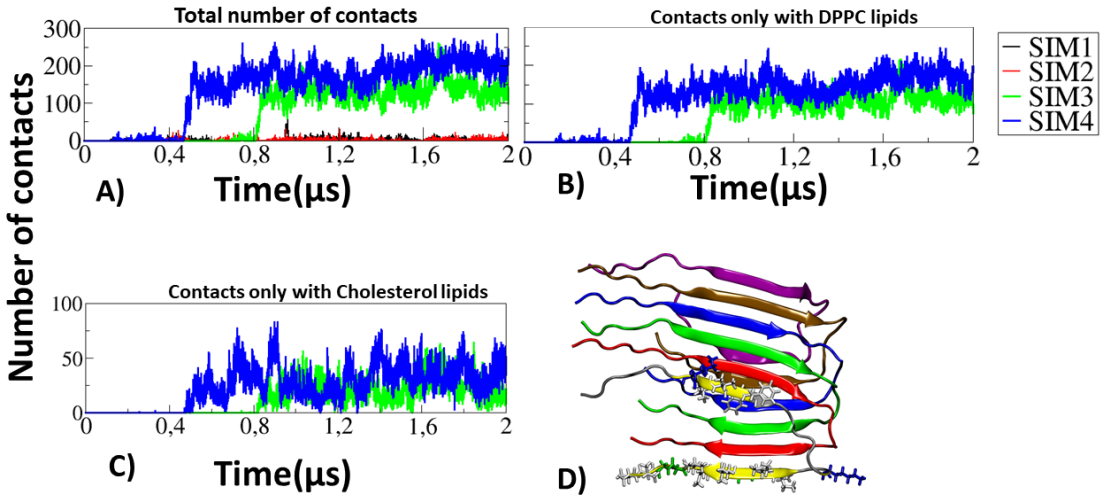

Figure 6. A) Time evolution of the number of contacts between the $A\beta_{9\text{-}40}$ fibril and both lipids, DPPC and cholesterol. B) Time evolution of the number of contacts between the $A\beta_{9\text{-}40}$ fibril and DPPC only. C) Time evolution of the number of contacts between the $A\beta_{9\text{-}40}$ fibril and cholesterol only. D) Membrane-binding residues of chain A of the $A\beta_{9\text{-}40}$ fibril are highlighted in yellow.

Perturbation of the thickness of the membrane bilayer

Previous experimental studies have revealed that peptide/protein binding on the surface of membranes cause membrane thinning and that further insertion of peptides inside the membrane could also lead to the formation of pores [32]. To investigate the effect of the binding of $A\beta_{9\text{-}40}$ fibrils on the membrane, we calculated the thickness of the cholesterol-rich

DPPC bilayer for all four independent trajectories at five different time points: 0-0.1µs, 0.4-05 µs, 0.9-1 µs, 1.4-1.5 µs, and 1.9-2.0 µs (Figure 7). As negligible or almost no binding between the $A\beta_{9-40}$ fibril and the membrane took place in SIM1 and SIM2, no localized change in thickness was observed at any point of the membrane in these two simulations. However, localized changes in thickness due to fibril binding were observed in SIM3 and SIM4. In particular, major localized thinning took place in SIM4 at the 1.4-1.5 µs and at the 1.9-2.0 µs time points. In the latter, thinning of the membrane caused an increase in the thickness of the rest of the membrane, suggesting that a local perturbation in lipid distribution in the membrane takes place upon binding. Overall these data suggest that binding of $A\beta_{9-40}$ fibrils could lead to a localized change in the thickness of the membrane, as observed in SIM4. In our study, the Aβ fibril consists of 6 peptides; however, *in-vivo*, the number of Aβ peptides that interact with the membrane would be much higher in number, which may lead to a more pronounced thinning of the membrane.

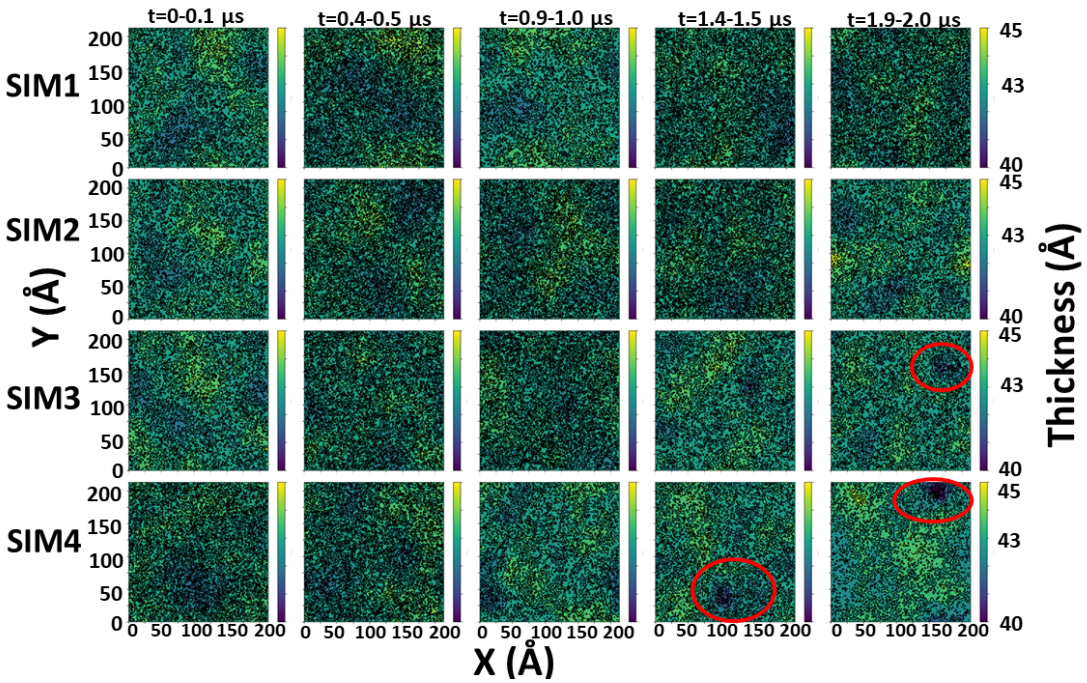

Figure 7. A) Thickness of the membrane in SIM1 at five different time points. B) Thickness of the membrane in SIM2 at five different time points C) Thickness of the membrane in SIM3 at five different time points. D) Thickness of the membrane in SIM4 at five different time points.

Discussion & Conclusions

In this study, we performed coarse-grained MD simulations of the interaction between an $A\beta_{9-40}$ fibril and a cholesterol-rich DPPC bilayer. Our simulation trajectories captured spontaneous binding of aqueous phase $A\beta_{9-40}$ fibril with the membrane. Indeed, highly negative interaction energy values showed that the binding between the membrane and $A\beta_{9-40}$ fibrils is favourable. This data is in agreement with the previous CG study of Dias *et al.* [18], which showed spontaneous favourable binding of $A\beta_{1-42}$ fibrils with membranes. Our simulations data reveals that both charged and hydrophobic residues participate in the binding with the membrane, in agreement also with previous studies reporting that both basic and hydrophobic amino acid residues play an important role in peripheral protein binding with the membranes [33, 34]. We also observed a loss of water molecules and an increase in the number of lipid molecules in the vicinity of the $A\beta_{9-40}$ fibril upon membrane binding. Moreover, at the position where $A\beta_{9-40}$ fibril bound to the membrane, localized thinning in the membrane was observed. The phenomena of membrane thinning by proteins and peptides inserting into the lipid bilayer are well established [35]. In *in-vivo* settings, where a significantly higher number of amyloid fibrils interact with the membrane, it is likely that their thinning effect on the membrane may increase significantly, which might result in pore formation or in the disruption of the membrane, leading to cytotoxicity [32].

In summary, our simulations have shed light on the mechanism of $A\beta_{9-40}$ fibril interaction with the membrane. To the best of our knowledge, this is the first report where spontaneous binding of $A\beta_{9-40}$ fibrils with a cholesterol-rich DPPC bilayer is shown. We identified key binding residues that stabilize the interaction of the $A\beta_{9-40}$ fibril with the membrane. These residues could guide the design of new drug candidates that could inhibit the association of $A\beta_{9-40}$ fibrils with the membrane, thus opening new avenues in the design of inhibitors of the Aβ peptide-lipid membrane interaction.

Acknowledgments

N.A. acknowledges the ERDF postdoc grant (No. 1.1.1.2/VIAA/4/20/757) for funding. E.P. thanks the ERDF project BioDrug (No. 1.1.1.5/19/A/004) and the Latvian Council of Science (grant No. lzp-2020/2-0013) for financial support. We would like to thank Latvian Institute of Organic Synthesis for computational resources. N.A. would also like to thank the Centre for

High Performance Computing (CHPC) in Cape Town (South Africa) for supercomputing resources.

Conflict of interest

The authors declare no competing interests.

References

[1] C.M. Dobson, T.P. Knowles, M. Vendruscolo, The amyloid phenomenon and its significance in biology and medicine, Cold Spring Harbor perspectives in biology, 12 (2020) a033878.
[2] C.M. Dobson, The amyloid phenomenon and its links with human disease, Cold Spring Harbor perspectives in biology, 9 (2017) a023648.
[3] F. Chiti, C.M. Dobson, Protein misfolding, amyloid formation, and human disease: a summary of progress over the last decade, Annu. Rev. Biochem, 86 (2017) 27-68.
[4] N. Agrawal, E. Parisini, Early stages of misfolding of PAP248-286 at two different pH values: An insight from molecular dynamics simulations, Computational and Structural Biotechnology Journal, 20 (2022) 4892-4901.
[5] I.Y. Quiroga, A.E. Cruikshank, M. Bond, K. Reed, B.A. Evangelista, J.-H. Tseng, J.V. Ragusa, R.B. Meeker, H. Won, S. Cohen, Synthetic amyloid beta does not induce a robust transcriptional response in innate immune cell culture systems, Journal of neuroinflammation, 19 (2022) 1-12.
[6] A.-M. Chiorcea-Paquim, A.M. Oliveira-Brett, Amyloid beta peptides electrochemistry: A review, Current Opinion in Electrochemistry, 31 (2022) 100837.
[7] T. Wu, D. Lin, Y. Cheng, S. Jiang, M.W. Riaz, N. Fu, C. Mou, M. Ye, Y. Zheng, Amyloid Cascade Hypothesis for the Treatment of Alzheimer's Disease: Progress and Challenges, AGING AND DISEASE, (2022).
[8] A. Mullard, Alzheimer amyloid hypothesis lives on, Nature Reviews Drug Discovery, 16 (2017) 3-5.
[9] R. Harrison, P. Sharpe, Y. Singh, D. Fairlie, Amyloid peptides and proteins in review, in: Reviews of physiology, biochemistry and pharmacology, Springer, 2007, pp. 1-77.
[10] M.M. Rahman, C. Lendel, Extracellular protein components of amyloid plaques and their roles in Alzheimer's disease pathology, Molecular Neurodegeneration, 16 (2021) 1-30.
[11] S. Han, M. Kollmer, D. Markx, S. Claus, P. Walther, M. Fändrich, Amyloid plaque structure and cell surface interactions of β-amyloid fibrils revealed by electron tomography, Scientific Reports, 7 (2017) 43577.
[12] J. Kiskis, H. Fink, L. Nyberg, J. Thyr, J.-Y. Li, A. Enejder, Plaque-associated lipids in Alzheimer's diseased brain tissue visualized by nonlinear microscopy, Scientific reports, 5 (2015) 13489.
[13] M.P. Burns, W.J. Noble, V. Olm, K. Gaynor, E. Casey, J. LaFrancois, L. Wang, K. Duff, Co-localization of cholesterol, apolipoprotein E and fibrillar Aβ in amyloid plaques, Molecular Brain Research, 110 (2003) 119-125.
[14] X. Yu, Q. Wang, Q. Pan, F. Zhou, J. Zheng, Molecular interactions of Alzheimer amyloid-β oligomers with neutral and negatively charged lipid bilayers, Physical Chemistry Chemical Physics, 15 (2013) 8878-8889.
[15] F. Tofoleanu, N.-V. Buchete, Molecular interactions of Alzheimer's Aβ protofilaments with lipid membranes, Journal of molecular biology, 421 (2012) 572-586.
[16] F. Tofoleanu, B.R. Brooks, N.-V. Buchete, Modulation of Alzheimer's Aβ protofilament-membrane interactions by lipid headgroups, ACS chemical neuroscience, 6 (2015) 446-455.
[17] X. Dong, Y. Sun, G. Wei, R. Nussinov, B. Ma, Binding of protofibrillar Aβ trimers to lipid bilayer surface enhances Aβ structural stability and causes membrane thinning, Physical Chemistry Chemical Physics, 19 (2017) 27556-27569.
[18] C.L. Dias, S. Jalali, Y. Yang, L. Cruz, Role of Cholesterol on Binding of Amyloid Fibrils to Lipid Bilayers, The Journal of Physical Chemistry B, 124 (2020) 3036-3042.
[19] M. Fändrich, S. Nyström, K.P.R. Nilsson, A. Böckmann, H. LeVine III, P. Hammarström, Amyloid fibril polymorphism: a challenge for molecular imaging and therapy, Journal of Internal Medicine, 283 (2018) 218-237.
[20] A.K. Paravastu, R.D. Leapman, W.-M. Yau, R. Tycko, Molecular structural basis for polymorphism in Alzheimer's β-amyloid fibrils, Proceedings of the National Academy of Sciences, 105 (2008) 18349-18354.

[21] S. Jo, T. Kim, V.G. Iyer, W. Im, CHARMM-GUI: a web-based graphical user interface for CHARMM, Journal of computational chemistry, 29 (2008) 1859-1865.
[22] Y. Qi, H.I. Ingólfsson, X. Cheng, J. Lee, S.J. Marrink, W. Im, CHARMM-GUI martini maker for coarse-grained simulations with the martini force field, Journal of chemical theory and computation, 11 (2015) 4486-4494.
[23] D.H. de Jong, G. Singh, W.D. Bennett, C. Arnarez, T.A. Wassenaar, L.V. Schafer, X. Periole, D.P. Tieleman, S.J. Marrink, Improved parameters for the martini coarse-grained protein force field, Journal of chemical theory and computation, 9 (2013) 687-697.
[24] S.J. Marrink, H.J. Risselada, S. Yefimov, D.P. Tieleman, A.H. De Vries, The MARTINI force field: coarse grained model for biomolecular simulations, The journal of physical chemistry B, 111 (2007) 7812-7824.
[25] M. Bixon, S. Lifson, Potential functions and conformations in cycloalkanes, Tetrahedron, 23 (1967) 769-784.
[26] H. Berendsen, J. Postma, W. van Gunsteren, A. Dinola, J. Haak, 571 1984. Molecular-dynamics with coupling to an external bath, J. Chem. Phys, 81 3684-3572.
[27] G. Bussi, D. Donadio, M. Parrinello, Canonical sampling through velocity rescaling, The Journal of chemical physics, 126 (2007) 014101.
[28] T. Darden, D. York, L. Pedersen, Particle mesh Ewald: An N· log (N) method for Ewald sums in large systems, The Journal of chemical physics, 98 (1993) 10089-10092.
[29] M.J. Abraham, T. Murtola, R. Schulz, S. Páll, J.C. Smith, B. Hess, E. Lindahl, GROMACS: High performance molecular simulations through multi-level parallelism from laptops to supercomputers, SoftwareX, 1 (2015) 19-25.
[30] N. Castillo, L. Monticelli, J. Barnoud, D.P. Tieleman, Free energy of WALP23 dimer association in DMPC, DPPC, and DOPC bilayers, Chemistry and physics of lipids, 169 (2013) 95-105.
[31] P. Bharadwaj, T. Solomon, C.J. Malajczuk, R.L. Mancera, M. Howard, D.W. Arrigan, P. Newsholme, R.N. Martins, Role of the cell membrane interface in modulating production and uptake of Alzheimer's beta amyloid protein, Biochimica et Biophysica Acta (BBA)-Biomembranes, 1860 (2018) 1639-1651.
[32] S.M. Butterfield, H.A. Lashuel, Amyloidogenic protein–membrane interactions: mechanistic insight from model systems, Angewandte Chemie International Edition, 49 (2010) 5628-5654.
[33] E. Fuglebakk, N. Reuter, A model for hydrophobic protrusions on peripheral membrane proteins, PLoS computational biology, 14 (2018) e1006325.
[34] A.H. Larsen, L.H. John, M.S. Sansom, R.A. Corey, Specific interactions of peripheral membrane proteins with lipids: what can molecular simulations show us?, Bioscience Reports, 42 (2022) BSR20211406.
[35] P.V. Bashkirov, P.I. Kuzmin, J. Vera Lillo, V.A. Frolov, Molecular shape solution for mesoscopic remodeling of cellular membranes, Annual review of biophysics, 51 (2022) 473-497.